Tonic activation of GLU_{K5} kainate receptors decreases neuroblast migration in whole-mounts of the subventricular zone

Jean-Claude Platel, Tristan Heintz, Stephanie Young, Valerie Gordon and Angélique Bordey

Departments of Neurosurgery, and Cellular & Molecular Physiology, Yale University, New Haven, CT 06520-8082, USA

In the postnatal subventricular zone (SVZ), neuroblasts migrate in chains along the lateral ventricle towards the olfactory bulb. AMPA/kainate receptors as well as metabotropic glutamate receptors subtype 5 (mGluR5) are expressed in SVZ cells. However, the cells expressing these receptors and the function of these receptors remain unexplored. We thus examined whether SVZ neuroblasts express mGluR5 and Ca^{2+}-permeable kainate receptors in mouse slices. Doublecortin (DCX)-immunopositive cells (i.e. neuroblasts) immunostained positive for mGluR5 and GLU_{K5-7}-containing kainate receptors. RT-PCR from ∼10 GFP-fluorescent cell aspirates obtained in acute slices from transgenic mice expressing green fluorescent protein (GFP) under the DCX promoter showed mGluR5 and GLU_{K5} receptor mRNA in SVZ neuroblasts. Patch-clamp data suggest that ∼60% of neuroblasts express functional GLU_{K5}-containing receptors. Activation of mGluR5 and GLU_{K5}-containing receptors induced Ca^{2+} increases in 50% and 60% of SVZ neuroblasts, respectively, while most neuroblasts displayed $GABA_A$-mediated Ca^{2+} responses. To examine the effects of these receptors on the speed of neuroblast migration, we developed a whole-mount preparation of the entire lateral ventricle from postnatal day (P) 20–25 DCX-GFP mice. The $GABA_A$ receptor ($GABA_AR$) antagonist bicuculline increased the speed of neuroblast migration by 27%, as previously reported in acute slices. While the mGluR5 antagonist MPEP did not affect the speed of neuroblast migration, the homomeric and heteromeric GLU_{K5} receptor antagonists, NS3763 and UB302, respectively, increased the migration speed by 38%. These data show that although both GLU_{K5} receptor and mGluR5 activations increase Ca^{2+} in neuroblasts, only GLU_{K5} receptors tonically reduce the speed of neuroblast migration along the lateral ventricle.

(Received 25 April 2008; accepted after revision 18 June 2008; first published online 19 June 2008)
Corresponding author A. Bordey: Department of Neurosurgery, Yale University School of Medicine, 333 Cedar Street, FMB 422, New Haven, CT 06520-8082, USA. Email: angelique.bordey@yale.edu

Neurogenesis persists in two regions of the adult brain, the subventricular zone (SVZ) along the lateral ventricle and the subgranular zone (SGZ) in the hippocampal dentate gyrus (Lledo *et al.* 2006). In the SVZ, neural progenitors expressing glial fibrillary acidic protein (GFAP) generate intermediate progenitors called transit amplifying progenitors. The latter generate neuroblasts that differentiate into interneurons in the olfactory bulb. Neuroblasts born in the SVZ migrate in chains along the lateral wall of the lateral ventricle. These chains surrounded by GFAP cells join to form a rostral migratory stream (RMS) reaching the olfactory bulb.

Signalling molecules exert strong controls over the different stages of cell development in adult neurogenic zones (Lledo *et al.* 2006). Some of these signals include the neurotransmitters GABA and glutamate. GABA has received particular attention perhaps because of the almost ubiquitous presence of $GABA_ARs$ on immature cells. GABA acting at $GABA_ARs$ exerts several effects on SVZ cells (Bordey, 2006, 2007), including a tonic reduction of the proliferation of GFAP cells (Liu *et al.* 2005) as well as the speed of neuroblast migration (Bolteus & Bordey, 2004). By comparison, the function of glutamate on SVZ neuroblast development has received little attention. Nevertheless, several elements of glutamatergic signalling are in place in the SVZ; glutamate immunostaining is intense in GFAP cells compared to neuroblasts (Platel *et al.* 2007*b*). GFAP cells express high affinity glutamate transporters GLAST and GLT-1 (Liu *et al.* 2006). Functional mGluR5 and AMPA/kainate receptors are also expressed in SVZ cells (Di Giorgi Gerevini *et al.* 2004; Platel

This paper has online supplemental material.

 DOI: 10.1113/jphysiol.2008.155879

et al. 2007*b*). In addition, pharmacological inhibition of mGluR5 *in vivo* was reported to decrease the number of proliferative cells in the SVZ (Di Giorgi-Gerevini *et al.* 2005). However, it remains unknown which SVZ cell types express mGluR5 and which type of AMPA and/or kainate receptors are present in neuroblasts. Kainate receptors exist as multiple subtypes with distinct functions and are composed of $GLU_{K5\text{-}7}$, GLU_{K1} and GLU_{K2} subunits (IUPHAR nomenclature of the receptors also known as GluR5-7, KA1 and KA2; Lerma *et al.* 2001; Pinheiro & Mulle, 2006). $GLU_{K5\text{-}7}$ either alone or in combination with GLU_{K1} or GLU_{K2} subunits form functional ion channels. Homomeric GLU_{K1} or GLU_{K2} receptors bind kainate with high affinity, but do not form functional ion channels. Tonic activation of GLU_{K5}-containing kainate receptors has been shown to influence later stages of cell development (e.g. synaptogenesis) (Lauri *et al.* 2006; Vesikansa *et al.* 2007). However, their function in early stages of cell development (e.g. migration) remains unexplored.

Here, we examined whether SVZ neuroblasts express functional mGluR5 and GLU_{K5}-containing kainate receptors. We then tested whether tonic activation of mGluR5 and GLU_{K5}-containing kainate receptors regulates the speed of neuroblast migration using time-lapse imaging of acute whole-mounts of the lateral ventricle.

Methods

Animals

Experiments were performed in FVB/N, C57BL6 and CD1 mice (Charles River, USA) and DCX-GFP (FVB/N background, kind gift from Dr R. Miller, University of Chicago, originally Gensat, USA). Immunostaining was performed in P30 FVB/N mice. Ca^{2+} imaging and patch-clamp recordings were performed in P19–30 CD1 and C57BL6 mice. Migration studies were performed in P20–25 DCX-GFP mice. All of the following experiments involving the above-described mice were carried out in accordance with the Yale Animal Care and Use Committee guidelines.

Immunohistochemistry

Mice were deeply anaesthetized with pentobarbital ($50\,mg\,kg^{-1}$ via intraperitoneal injection) and decapitated. The brains were quickly removed and placed in 4% paraformaldehyde overnight at 4°C. Free-floating coronal slices, 100 μm thick, were blocked in Tris-buffered saline (TBS) containing 0.1% Triton X-100 + 0.1% Tween-20 + 2% BSA, and incubated in the primary antibodies overnight at 4°C as previously described (Platel *et al.* 2007*b*): anti-DCX (goat or rabbit, 1 : 100, Santa Cruz); anti-GFAP-Cy3 (mouse IgG1, 1 : 500, Sigma); anti-GLAST (guinea pig, 1 : 1000), anti-mGluR5 (rabbit, 1 : 500), and anti-$GLU_{K5\text{-}7}$ (mouse IgGM, 1 : 500, Chemicon). After several washes, slices were incubated with the appropriate secondary antibodies (Alexa Fluor series at 1 : 1000, Invitrogen, or cyanine series at 1 : 500, Jackson Laboratories) for 1 h at room temperature.

Z-stack images (spaced by 0.5–2 μm over 10–20 μm) were acquired on a confocal microscope (Olympus FluoView 1000) with a ×20 dry objective (NA 0.75) or a ×60 oil objective (NA 1.42). Images were analysed using Imaris 4.0 (Bitplane AG) and reconstructed in ImageJ (Freeware, Wayne Rasband, NIH) and Photoshop CS3.

RT-PCR

Approximately 10 GFP-positive cells were aspirated into a patch pipette from an acute coronal slice from a DCX-GFP mouse. The solution was ejected into 10 μl of resuspension buffer containing 40 units of RNaseOUT (Invitrogen). Reverse transcription (RT) was conducted using Superscript III (Invitrogen). Samples were treated with RNaseH for 20 min at 37°C then kept on ice until the PCR. The PCR was conducted using the AccuPrime high yield *Taq* DNA Polymerase System (Invitrogen) and selective primers for GLU_{K5} and mGluR5. GLU_{K5} primers: forward: CCCTGACTCAGACGTGGTGGAA; reverse: AGAAGGTCATTGTCGAGCCATCTC; forward nested: GTTGGAGCTCTCATGCAGCAAGG; reverse nested: AGAAGGTCATTGTCGAGCCATCTC (product size: 234 bp). mGluR5 primers: forward GTCCTTCTGTTGATCCTGTC; reverse: ATGCAGCATGGCCTCCACTC (product size: 216 bp). Thirty PCR cycles were run; 2 μl of the PCR product was added to fresh mastermix and primers to run for an additional 40 cycles. The product was resolved on 2% agarose gel in TAE buffer.

Patch-clamp recordings and Ca^{2+} imaging in acute slices

Acute sagittal brain slices (300 μm thick) containing the SVZ were prepared as we have previously described (Bolteus & Bordey, 2004). Cells were visualized with an upright Olympus BX61WI microscope equipped with an Olympus FluoView 1000 confocal system and a water-immersion fluorescence ×60 objective (NA 0.9). Slices were superfused with oxygenated artificial cerebrospinal fluid (aCSF) for patch-clamp recordings or high glucose Dulbecco's modified Eagle medium (DMEM) for Ca^{2+} imaging. aCSF contains (in mM): NaCl 125; KCl 2.5; $CaCl_2$ 1.8; $MgCl_2$ 1; $NaHCO_3$ 25; glucose 10.

Perforated patch-clamp recordings using gramicidin (5 μg ml^{-1}) were obtained as we previously described (Wang *et al.* 2003*a*,*b*). The intracellular solution contained KCl 140; $CaCl_2$ 1.0; $MgCl_2$ 2.0; EGTA 10; Hepes 10; pH adjusted to 7.2 with KOH. Filled patch pipettes had a resistance of 8–10 MΩ. An Axopatch 200B amplifier, Digidata 1322A digitizer, and pCLAMP10 software (Axon Instruments) were used for recordings (2 kHz low-pass filtered; 5 kHz sampling rate). No correction of junction potentials was performed. Half of the recordings were performed following incubation in concanavalin A (25–30 min, 10–20 μM), a lectin protein that eliminates kainate receptor desensitization. No differences were found between cells with or without concanavalin A pre-treatment.

For Ca^{2+} imaging, SVZ cells were loaded by either bath (45 min in 10 μM fluo4-AM) or pressure application of fluo4-AM (250 μM in DMEM). The frequency of cytosolic Ca^{2+} increases was calculated using Calsignal (Platel *et al.* 2007*a*). Images were acquired every 1.16–3 s with FluoView acquisition software. F_0 (i.e. baseline) is the mean fluorescence intensity measured throughout all the regions of interest, and F is the mean fluorescence intensity in a single cell. A change in fluorescence was considered to be a Ca^{2+} increase if $> 15\%$ F/F_0. Ca^{2+} data were collected in > 3 slices from > 3 mice; 19–203 cells were analysed per slice.

Analysis of the speed of migration in whole-mounts of the SVZ

For preparing whole-mounts, the entire brain was placed in cold, oxygenated high sucrose aCSF under a dissecting microscope. After removal of the cerebellum, a medial incision was performed between the two hemispheres. The lateral ventricle was opened through its dorso-medial part, and by peeling away the corpus callosum and cortex. The tissue located ventrally to the lateral ventricle, as well as the anterior and posterior ends, was dissected out. The hippocampus was then removed, making the entire lateral ventricle visible. The choroid plexus, cortex and corpus callosum were dissected out.

Migration movies were acquired at 37°C on the Olympus confocal microscope with a Super ×20 dry objective (NA 0.95) in high glucose DMEM using whole-mounts of the lateral ventricle. For each drug treatment, the migration speed was measured in > 3 whole-mounts from three mice. At least six movies were acquired per drug: three movies under control conditions followed by a 30 min wash-in period for a drug, and three movies with the drug. Each movie was 1 h long and contained 12 image stacks spaced by 5 min. Each image stack was a series of 2 μm-spaced Z-sections over 30–80 μm. More than 10 neuroblasts in chains were analysed per movie. Image stacks were realigned and GFP-fluorescent cells were tracked using ImageJ plug-ins (Stackreg and MTrackJ, respectively).

Receptor agonists and antagonists were applied by pressure and bath, respectively. Drugs were from Tocris except when noted. Data are expressed as mean ± S.E.M. Statistical analysis used a two-tailed t test unless noted. Significance was set at $P < 0.05$.

Results

mGluR5 and GLU_{K5-7} kainate receptors are expressed in SVZ neuroblasts

Co-immunostaining was performed for selective glutamate receptors and either the microtubule-associated protein DCX (Fig. 1*A* and *B*), a neuroblast marker (Nacher *et al.* 2001), or the glutamate/aspartate transporter (GLAST) or GFAP, two astrocytic markers (Bolteus & Bordey, 2004; Liu *et al.* 2006). mGluR5 immunofluorescence (green) is visible in DCX-immunopositive cells (red, Fig. 1*A* and *B*, yellow arrow) as well as in presumed ependymal cells (Fig. 1*A*, white arrow). By contrast, GLAST-positive cells (blue) do not co-stain for mGluR5 (Fig. 1*B*, yellow arrowhead). Using an antibody that recognizes GLU_{K5-7} kainate receptors (Siegel *et al.* 1995), we found that staining for these receptors (green) is present in DCX-positive cells (red, Fig. 1*C* and *D*, white arrow) as well as faintly in some GFAP-positive cells (blue, Fig. 1*D*, yellow arrow). However, most of the GFAP-positive cells do not display GLU_{K5-7} receptor staining. These data suggest that neuroblasts express both mGluR5 and GLU_{K5-7}-containing receptors. Nevertheless, some DCX-positive cells did not co-stain for either mGluR5 or GLU_{K5-7} receptors (green, Fig. 1*B* and *D*, white arrowheads), suggesting heterogeneity in their glutamate receptor expression. To further examine whether neuroblasts express mGluR5 or GLU_{K5-7} receptors, we performed RT-PCR from aspirates of GFP-fluorescent cells from acute DCX-GFP slices. GLU_{K5} and mGluR5 mRNA were detected in aspirates of ∼10 neuroblasts (Fig. 1*E* and *F*).

Neuroblasts display kainate receptor-mediated currents

Kainate receptors are ionotropic glutamate receptors whose activation can lead to inward currents in cells recorded with the patch-clamp technique. To test whether kainate receptors in neuroblasts were functional, perforated patch-clamp recordings were obtained from SVZ cells along the lateral side of the lateral ventricle in acute sagittal slices. Recorded cells were maintained at a holding potential of –60 mV (near their physiological

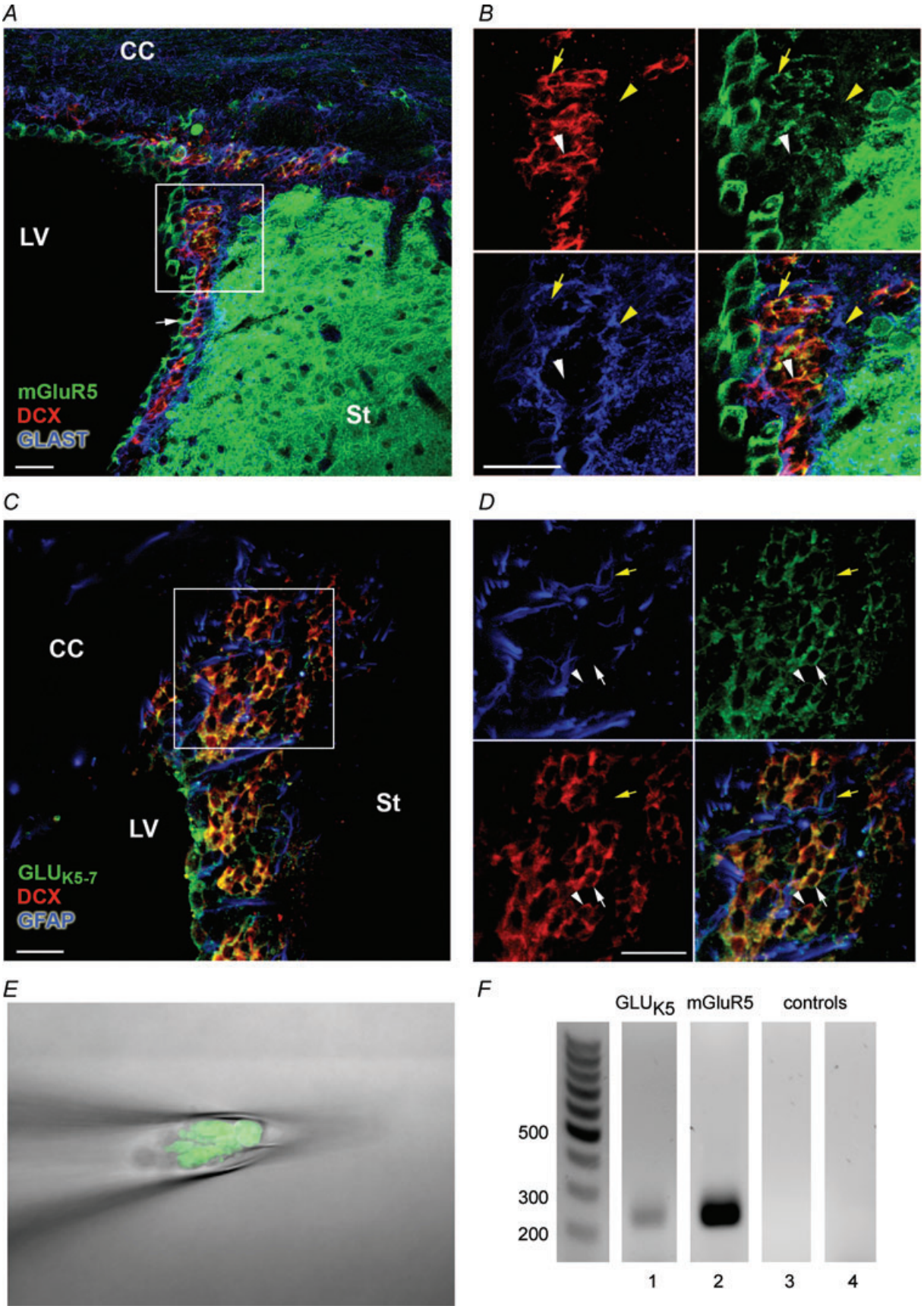

resting potentials) and were identified as neuroblasts based on their biophysical properties and current profiles (Wang *et al.* 2003*a*,*b*). Recordings were performed in the presence of a $GABA_A$R blocker (50 μM bicuculline) to avoid current contamination by baseline $GABA_A$R channel activity. Pressure application of a broad-spectrum kainate receptor agonist, domoate (10 μM), induced inward currents of -3.6 ± 0.8 pA in 70% of recorded neuroblasts ($n = 7/10$, Fig. 2*A*). To activate more selectively GLU_{K5} receptors, we pressure applied an agonist of GLU_{K5}-containing kainate receptors, ATPA (10–25 μM) (Hoo *et al.* 1999). ATPA also acts as a partial agonist for a $GLU_{K6/K2}$ receptors (Paternain *et al.* 2000; Alt *et al.* 2004; Christensen *et al.* 2004*a*). ATPA (10–20 s) induced an increase in baseline noise or single channel activity in 56% of SVZ neuroblasts ($n = 14/25$, Fig. 2*B* and *C*). ATPA-induced single channels displayed a mean amplitude of -0.9 ± 0.2 pA ($n = 207$ events, 5 neuroblasts, ranging from –0.40 to –1.58 pA, Fig. 2*D*). Events < 0.5 pA were difficult to resolve from the noise and are underestimated. A Gaussian fit of the amplitude histogram (bin size: 0.12 pA) obtained from these ATPA-induced single channels also gave a mean amplitude of –0.9 pA ($r^2 = 0.96$, Fig. 2*E*). This mean channel amplitude suggests the presence of unedited GLU_{K5}-containing or $GLU_{K6/K2}$-containing receptors (Howe, 1996; Swanson *et al.* 1996) in ~60% of SVZ neuroblasts. We next used Ca^{2+} imaging to examine ATPA responses and test the effects of antagonists.

SVZ neuroblasts coexpress GLU_{K5}-containing kainate receptors, mGluR5 and $GABA_A$Rs

Cells in the lateral SVZ (i.e. along the lateral ventricle) were loaded with the high affinity Ca^{2+} indicator fluo4-AM in acute, rostral coronal slices (Bregma anteroposterior 0–1). Pressure application of ATPA (10–20 μM, 10 s) induced a $92.2 \pm 9.3\%$ transient Ca^{2+} increase in $59.9 \pm 3.8\%$ of SVZ cells ($n = 268$ cells, 3 slices, Fig. 3*A*–*E*, *G* and *H*). The change of fluorescence was measured at the peak response. ATPA applications spaced by 1 min induced reproducible Ca^{2+} increases with no apparent rundown (data not shown). Pressure application of control DMEM induced no change in Ca^{2+} in SVZ cells (data not shown). Considering that neuroblasts correspond to ~70% of the rostral SVZ cell population, these data suggest that ATPA induced Ca^{2+} increases in neuroblasts. We then tested the effects of two kainate receptor antagonists UBP302 and NS3763 on ATPA-induced Ca^{2+} responses. UBP302 is a competitive antagonist of GLU_{K5}-containing receptors, including homomeric and heteromeric forms (More *et al.* 2004; Dolman *et al.* 2005). NS3763 is a non-competitive antagonist selective for homomeric GLU_{K5} receptors (Christensen *et al.* 2004*a*,*b*). Bath application of UBP302 (10 μM) completely blocked ATPA-induced Ca^{2+} increases in $88.8 \pm 7.9\%$ of the responding cells ($n = 3$, 3 slices, Fig. 3*F*). NS3763 (25 μM) completely blocked ATPA-induced Ca^{2+} increases in $56.0 \pm 3.0\%$ of the responding cells ($n = 152$ cells, 3 slices, Fig. 3*D* and *F*). These data suggest the presence of homomeric, unedited GLU_{K5} receptors in 56% of SVZ cells.

mGluR5 belongs to the group I mGluRs, which also include mGluR1, and mobilizes Ca^{2+} from IP_3-regulated intracellular stores (Conn & Pin, 1997). To test whether mGluR5 were functional in SVZ neuroblasts, we pressure applied DHPG, a group I mGluR agonist. DHPG induced a $70.0 \pm 2.2\%$ Ca^{2+} increase in $43.0 \pm 2.0\%$ of SVZ cells ($n = 268$ cells, 3 slices, Fig. 3*E*, *G* and *H*). DHPG-induced Ca^{2+} increases were completely blocked by the selective mGluR5 antagonist MPEP (50 μM, Salt *et al.* 1999) in $62.6 \pm 10.0\%$ of responding cells ($n = 51$ cells, 3 slices, Fig. 3*F*), suggesting that neuroblasts express functional mGluR5.

In an effort to determine whether SVZ cells express GLU_{K5} receptors and mGluR5 as well as $GABA_A$Rs, selective agonists of each receptor type were successively applied on the same cells. The $GABA_A$R agonist isoguvacine (50 μM) induced transient Ca^{2+} increases in $80.1 \pm 7.4\%$ of SVZ cells ($n = 268$ cells, 3 slices, Fig. 3*G* and *H*) that were blocked by bath application of the $GABA_A$R antagonist, bicuculline (50 μM, $n = 142$ cells, 3 slices, data not shown). Of the GABA-sensitive SVZ cells, $31.9 \pm 2.9\%$ express both mGluR5 and GLU_{K5}-containing receptors (DHPG- and ATPA-sensitive cells, respectively); $9.1 \pm 1.3\%$ and $22.3 \pm 8.6\%$ of the GABA-sensitive cells express either mGluR5 or GLU_{K5}-containing receptors (Fig. 3*H*).

Figure 1. SVZ neuroblasts express mGluR5 and $GLU_{K5\text{-}7}$-containing kainate receptors
A and *B*, photographs of immunostaining for mGluR5 (green), DCX (red) and GLAST (blue) in a coronal section from a P30 mouse brain at low (*A*) and high magnification (*B*). mGluR5 (green) is expressed by neuroblasts (red, yellow arrow) and ependymal cells (white arrow in *A*), but not by GLAST-positive cells, i.e. astrocytes (blue, yellow arrowhead). *C* and *D*, photographs of immunostaining for $GLU_{K5\text{-}7}$-containing receptors (green), DCX (red) and GFAP (blue) in a coronal section from a P30 mouse brain at low (*C*) and high magnification (*D*). $GLU_{K5\text{-}7}$-containing receptors are expressed by neuroblasts (red, white arrow) and in a few GFAP cells (blue, yellow arrow). Some neuroblasts do not stain for $GLU_{K5\text{-}7}$-containing receptors (white arrowhead). Scale bars, 20 μm. *E* and *F*, agarose gel electrophoresis (*F*) demonstrating RT-PCR amplification of GLU_{K5} (lane '1') and mGluR5 (lane '2') mRNA isolated during pipette aspiration of 10 GFP-fluorescent cells, i.e. neuroblasts, shown in *E*. GLU_{K5} and mGluR5 were not detected in bath solution (lane '3' for GLU_{K5} and lane '4' for mGluR5) controls.

Collectively, these data suggest that nearly all SVZ neuroblasts express $GABA_A$Rs, while a subset expresses different types of glutamate receptors, including mGluR5, homomeric GLU_{K5} receptors, and other GLU_{K5}-containing receptors. There is thus a mosaic of glutamate receptor expression in SVZ neuroblasts.

Tonic activation of $GABA_A$Rs and GLU_{K5} receptors decreases the speed of neuroblast migration in whole-mounts of the SVZ

To assess the effects of drugs on the speed of neuroblast migration, we prepared acute whole-mounts of the lateral ventricle (Fig. 4*A*). This preparation has been used for immunostaining and examining the pattern of neuroblast chains. Indeed, chains of GFP-fluorescent neuroblasts are clearly visible and intact in a live whole-mount of the lateral ventricle from a DCX-GFP mouse (Fig. 4*A*). Time-lapse imaging was performed to determine the speed of neuroblast migration (Fig. 4*B* and *C*, see online Supplemental movie). During a 1 h movie, neuroblasts migrated at $66.3 \pm 2.4\ \mu m\ h^{-1}$ (ranging from 21 to $140\ \mu m\ h^{-1}$, $n = 18$ whole-mounts). The majority of the GFP-fluorescent cells migrated in chains. The migration speed was evaluated in rostral sections of the whole-mount to match regions recorded during

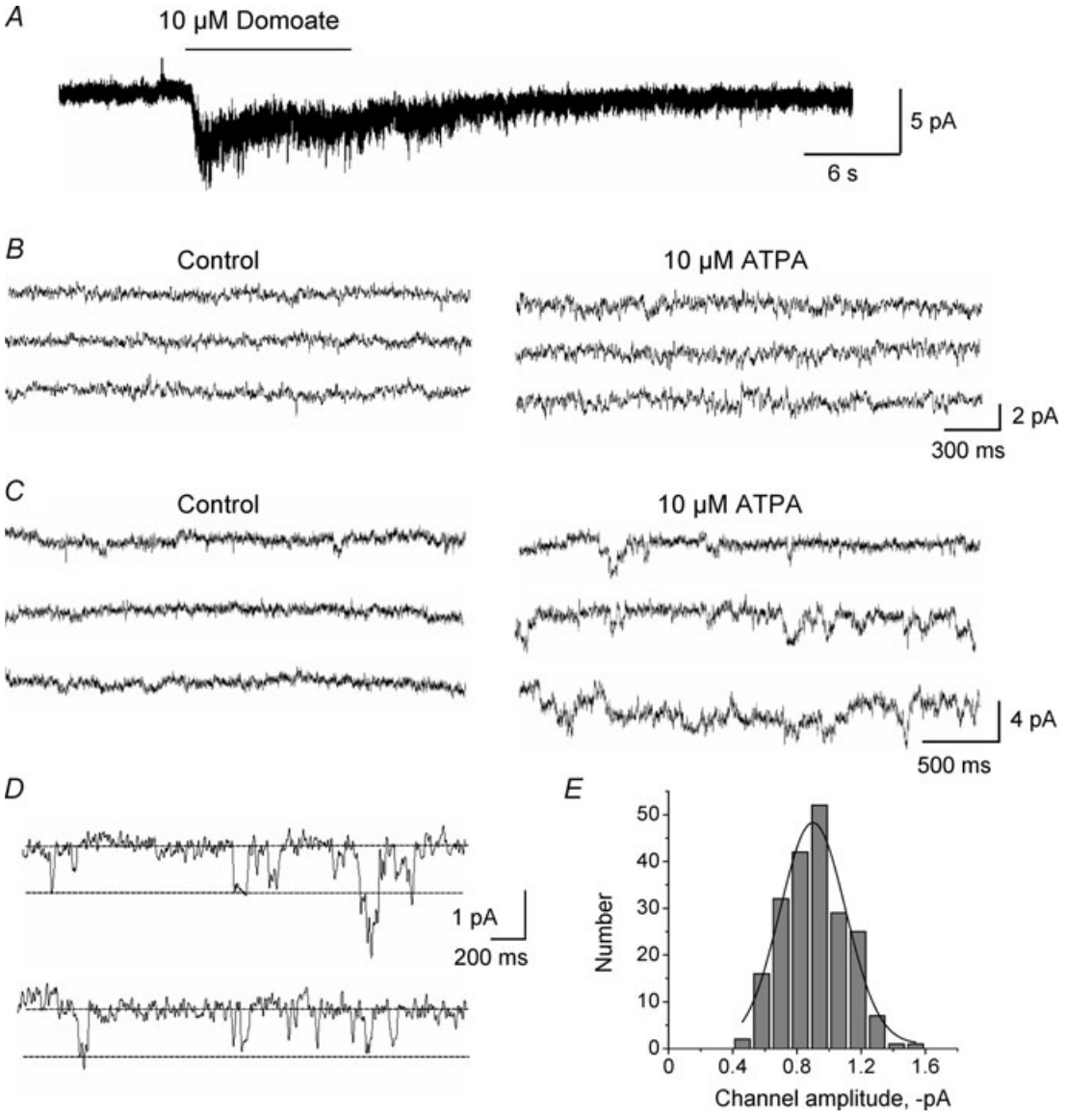

Figure 2. Kainate receptor channel activity in SVZ neuroblasts
A–C, representative traces from perforated patch-clamp records of SVZ neuroblasts. *A*, a broad-spectrum kainate receptor agonist domoate (10 μM, 10 s) induces an inward current in a SVZ neuroblast. *B* and *C*, the GLU_{K5}-containing receptor agonist ATPA (25 μM) increases baseline noise (*B*) or induces single-channel activity (*C*) in two different neuroblasts. *D*, higher resolution of ATPA-induced single channels in a neuroblast. *E*, amplitude histogram (bin size: 0.12 pA) of ATPA-induced single channels pooled from 5 neuroblasts.

Ca^{2+} imaging (Fig. 3). We previously reported that bicuculline (50 μM) increased the speed of SVZ neuroblast migration by 30% in acute sagittal slices (Bolteus & Bordey, 2004). Here, we also found that bicuculline (100 μM) increased the speed of neuroblast migration by 26.7% (from 66.5 ± 6.8 to 83.5 ± 6.2 μm h^{-1}; $P < 0.05$, $n = 3$ whole-mounts, Fig. 4*D*). We also measured the maximum speed reached during the 1 h recording for each cell and found that it increased by 10.6% with bicuculline (Fig. 4*E*). MPEP (50 μM, mGluR5 blocker) changed neither the

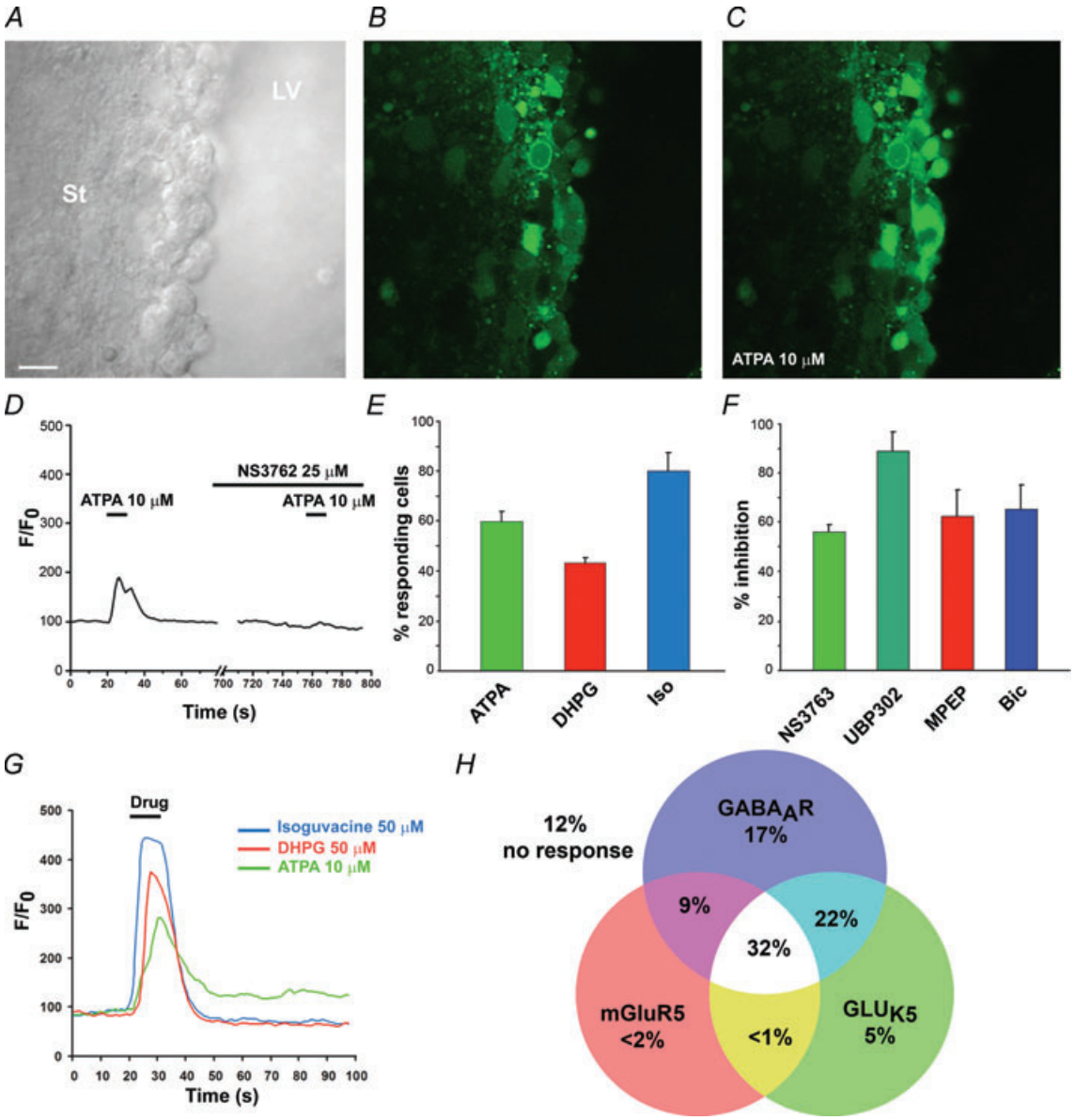

Figure 3. Activation of GLU_{K5} receptors, mGluR5 and $GABA_A$Rs increases Ca^{2+} in overlapping sub-populations of SVZ neuroblasts

A, DIC photograph of the lateral SVZ along the lateral ventricle (LV). Scale bar, 20 μm. St, striatum. *B*–*C*, photographs of fluo4 fluorescence in the same SVZ region as shown in *A* taken before (*B*) and after 10 μM ATPA application (*C*). Fluo4-AM was pressure-applied onto SVZ cells. *D*, a representative trace of normalized fluo4 fluorescence (from *B* and *C*) over time illustrates that ATPA-induced Ca^{2+} increases in SVZ cells were blocked by the non-competitive, homomeric GLU_{K5} inhibitor NS3763. *E*, bar graph illustrating the percentage of SVZ cells responding to ATPA, the mGluR5 agonist DHPG (50 μM), and the $GABA_A$R agonist isoguvacine (iso, 50 μM). *F*, bar graph illustrating the percentage inhibition of ATPA-, DHPG- and isoguvacine-induced Ca^{2+} responses by NS3763, UBP302, MPEP and bicuculline (Bic). UBP302 is a competitive blocker of GLU_{K5}-containing receptors. *G*, representative ATPA-, DHPG- and isoguvacine-induced Ca^{2+} increases in the same neuroblast. *H*, a Venn diagram illustrating the percentage of cells expressing one or a combination of the following receptors: GLU_{K5}, mGluR5 and $GABA_A$Rs.

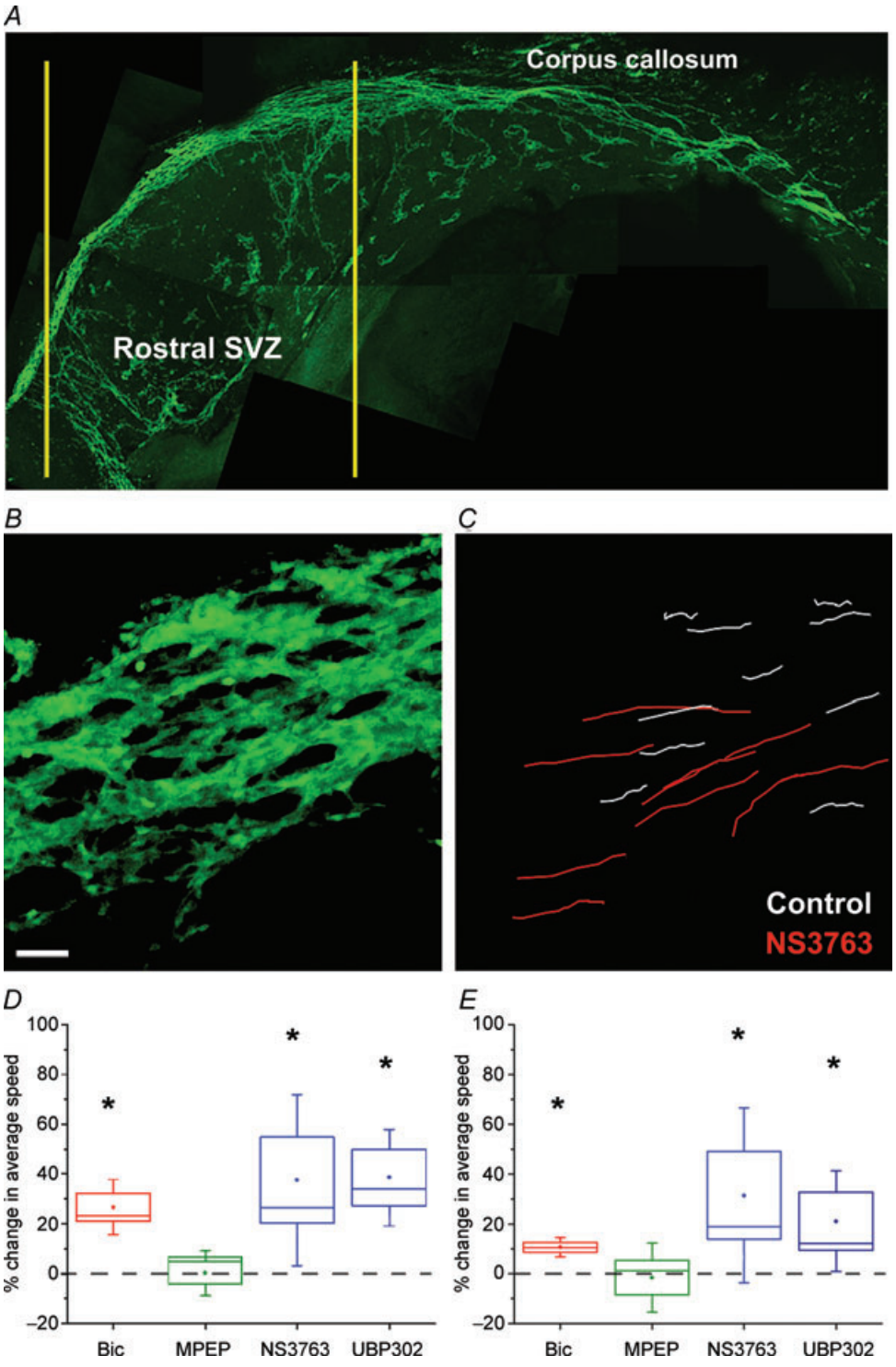

Figure 4. Tonic activation of $GABA_A$Rs and homomeric GLU_{K5} receptors decreases the speed of neuroblast migration in whole-mounts of the lateral ventricle
A, composite images of a fixed whole-mount from a P60 DCX-GFP mouse taken at ×10 magnification. The yellow lines indicate the region where the migration movies were acquired. Scale bar, 70 μm. *B*, a representative Z-stack image (25 Z sections spaced by 2 μm) of SVZ chains in a DCX-GFP whole-mount preparation. *C*, migratory routes of individual cells from the Z-stack image shown in *B* before (white lines) and during NS3763 application (red lines). Scale bar, 50 μm. *D*, bar graph illustrating the percentage change in the migration speed in the presence of bicuculline (50 μM), MPEP (50 μM), NS3763 (25 μM) or UBP302 (10 μM). * $P < 0.05$. *E*, bar graph illustrating the percentage change in the maximum speed of neuroblasts. In the plots in *D* and *E*: box, S.E.M.; whisker, S.D.; middle line, median.

migration speed nor the maximum speed. NS3763 (25 μM) significantly increased the speed of neuroblast migration by 37% (from 63.0 ± 3.1 to 85.0 ± 4.6 μm h^{-1}; $P < 0.05$, $n = 4$ whole-mounts, Fig. 4*B* and *D*). Similarly, UBP302 (10 μM, GLU_{K5}-containing receptor blocker) significantly increased the speed of neuroblast migration by 38.6% (from 60.0 ± 5.3 to 82.4 ± 5.3 μm h^{-1}; $P < 0.05$, $n = 3$ whole-mounts, Fig. 4*D*). The maximum speed of migration was also significantly increased by 21% (Fig. 4*E*, $P < 0.05$). DMSO (vehicle for NS3763), 0.1%, had no effect on the speed of neuroblast migration (67.2 ± 3.7 μm h^{-1} in control and 64.9 ± 6.4 μm h^{-1} in DMSO, data not shown). Collectively, tonic activation of GLU_{K5} kainate receptor but not of mGluR decreases the speed of neuroblast migration (Fig. 1 in online Supplemental material).

Discussion

Here, we show for the first time that neuroblasts migrating in the SVZ express functional homomeric GLU_{K5} receptors. These kainate receptors are tonically activated by ambient glutamate resulting in a reduction of the speed of neuroblast migration. This is a novel function of GLU_{K5} receptors prior to synapse formation.

SVZ neuroblasts express a mosaic of glutamate receptors prior to synapse formation

We show the functional expression of mGluR5 and GLU_{K5} kainate receptors in SVZ neuroblasts. Our pharmacological data using NS3763 suggest that neuroblasts express homomeric GLU_{K5} receptors (Christensen *et al.* 2004*b*). This is the first report of functional, native homomeric GLU_{K5} receptors. ATPA-induced Ca^{2+} increases suggest that neuroblasts express unedited GLU_{K5} receptors, which display higher Ca^{2+} permeability than its edited counterpart (Kohler *et al.* 1993). This finding is in agreement with previous data showing that RNA editing is developmentally regulated (Bernard & Khrestchatisky, 1994). These data suggest the presence of homomeric GLU_{K5} receptors in neuroblasts, but do not preclude the expression of other types of kainate receptors. It is possible that neuroblasts express other GLU_{K5}-containing receptors (including $GLU_{K5/K6}$ or $GLU_{K5/K2}$) as well as $GLU_{K6/K2}$ receptors, since mRNA for all kainate receptor subunits has been shown in neuroblasts in the RMS of the olfactory bulb (Davila *et al.* 2007).

One remarkable finding was that not every neuroblast expresses the same subset of glutamate receptors. There are four major groups of neuroblasts expressing: (1) only $GABA_A$Rs, (2) $GABA_A$ and GLU_{K5} receptors, (3) $GABA_A$Rs and mGluR5, and (4) all three receptor types. These differences could be due to the 'age' or differentiation state of the imaged cells as some neuroblasts are born caudally to the recording site. Alternatively, neuroblasts may differ based on their ultimate fate in the olfactory bulb (Merkle *et al.* 2007).

GLU_{K5} receptor but not mGluR5 activation affects the speed of neuroblast migration

This is the first time that the whole-mount preparation has been used for studying live migration of SVZ neuroblasts. The average speed of neuroblast migration ($\sim$65 μm h^{-1}) is similar to that measured in acute sagittal slices ($\sim$50–70 μm h^{-1}; Bolteus & Bordey, 2004; Nam *et al.* 2007). Chains are organized and intact in whole-mounts, while they were either disorganized or truncated in slices. In addition, one clear difference with the slice preparation is the presence of an intact layer of ependymal cells, which may contribute to the regulation of neuroblast migration and prevent the loss of local factors.

Our experiments using bicuculline to block tonic $GABA_AR$ activation in whole-mounts validated our previous findings in acute slices (Bolteus & Bordey, 2004) and confirmed that $GABA_A$Rs are tonically activated in migrating neuroblasts. Although activation of either mGluR5 or GLU_{K5} receptors induced Ca^{2+} increases in neuroblasts, only inhibition of tonic GLU_{K5} receptor activation increased the speed of neuroblast migration while a mGluR5 blocker had no effect. Presumably each receptor type involves distinct intracellular cascades and messengers that differentially affect cell development. Mechanistically, it remains to be determined whether GLU_{K5} receptors act by affecting cell chemokinesis or chemotaxis, and whether intracellular Ca^{2+} changes are involved in this control. GLU_{K5} receptors have also been shown to act as metabotropic receptors via a G-protein-dependent mechanism (Pinheiro & Mulle, 2006). This is another possible mechanism that would need to be further explored. Finally, it is also possible that tonic GLU_{K5} activation via both intracellular Ca^{2+} increases and neuroblast depolarization promotes the release of GABA or another diffusible molecule resulting in a reduction of the speed of neuroblast migration.

Collectively, glutamate and GABA together or independently provide homeostatic controls on SVZ neuroblasts to properly regulate their production and migration (for review on glutamatergic signalling see Platel *et al.* 2008 in this issue).

References

Alt A, Weiss B, Ogden AM, Knauss JL, Oler J, Ho K, Large TH & Bleakman D (2004). Pharmacological characterization of glutamatergic agonists and antagonists at recombinant human homomeric and heteromeric kainate receptors in vitro. *Neuropharmacology* **46**, 793–806.

Bernard A & Khrestchatisky M (1994). Assessing the extent of RNA editing in the TMII regions of GluR5 and GluR6 kainate receptors during rat brain development. *J Neurochem* **62**, 2057–2060.

Bolteus AJ & Bordey A (2004). GABA release and uptake regulate neuronal precursor migration in the postnatal subventricular zone. *J Neurosci* **24**, 7623–7631.

Bordey A (2006). Adult neurogenesis: basic concepts of signaling. *Cell Cycle* **5**, 722–728.

Bordey A (2007). Enigmatic GABAergic networks in adult neurogenic zones. *Brain Res Brain Res Rev* **53**, 124–134.

Christensen JK, Paternain AV, Selak S, Ahring PK & Lerma J (2004*a*). A mosaic of functional kainate receptors in hippocampal interneurons. *J Neurosci* **24**, 8986–8993.

Christensen JK, Varming T, Ahring PK, Jorgensen TD & Nielsen EO (2004*b*). In vitro characterization of 5-carboxyl-2,4-di-benzamidobenzoic acid (NS3763), a noncompetitive antagonist of GLUK5 receptors. *J Pharmacol Exp Ther* **309**, 1003–1010.

Conn PJ & Pin JP (1997). Pharmacology and functions of metabotropic glutamate receptors. *Annu Rev Pharmacol Toxicol* **37**, 205–237.

Davila NG, Houpt TA & Trombley PQ (2007). Expression and function of kainate receptors in the rat olfactory bulb. *Synapse* **61**, 320–334.

Di Giorgi Gerevini V, Caruso A, Cappuccio I, Ricci Vitiani L, Romeo S, Della Rocca C, Gradini R, Melchiorri D & Nicoletti F (2004). The mGlu5 metabotropic glutamate receptor is expressed in zones of active neurogenesis of the embryonic and postnatal brain. *Brain Res Dev Brain Res* **150**, 17–22.

Di Giorgi-Gerevini V, Melchiorri D, Battaglia G, Ricci-Vitiani L, Ciceroni C, Busceti CL, Biagioni F, Iacovelli L, Canudas AM, Parati E, De Maria R & Nicoletti F (2005). Endogenous activation of metabotropic glutamate receptors supports the proliferation and survival of neural progenitor cells. *Cell Death Differ* **12**, 1124–1133.

Dolman NP, Troop HM, More JC, Alt A, Knauss JL, Nistico R, Jack S, Morley RM, Bortolotto ZA, Roberts PJ, Bleakman D, Collingridge GL & Jane DE (2005). Synthesis and pharmacology of willardiine derivatives acting as antagonists of kainate receptors. *J Med Chem* **48**, 7867–7881.

Hoo K, Legutko B, Rizkalla G, Deverill M, Hawes CR, Ellis GJ, Stensbol TB, Krogsgaard-Larsen P, Skolnick P & Bleakman D (1999). [^{3}H]ATPA: a high affinity ligand for GluR5 kainate receptors. *Neuropharmacology* **38**, 1811–1817.

Howe JR (1996). Homomeric and heteromeric ion channels formed from the kainate-type subunits GluR6 and KA2 have very small, but different, unitary conductances. *J Neurophysiol* **76**, 510–519.

Kohler M, Burnashev N, Sakmann B & Seeburg PH (1993). Determinants of Ca^{2+} permeability in both TM1 and TM2 of high affinity kainate receptor channels: diversity by RNA editing. *Neuron* **10**, 491–500.

Lauri SE, Vesikansa A, Segerstrale M, Collingridge GL, Isaac JT & Taira T (2006). Functional maturation of CA1 synapses involves activity-dependent loss of tonic kainate receptor-mediated inhibition of glutamate release. *Neuron* **50**, 415–429.

Lerma J, Paternain AV, Rodriguez-Moreno A & López-Garcia JC (2001). Molecular physiology of kainate receptors. *Physiol Rev* **81**, 971–998.

Liu X, Bolteus AJ, Balkin DM, Henschel O & Bordey A (2006). GFAP-expressing cells in the postnatal subventricular zone display a unique glial phenotype intermediate between radial glia and astrocytes. *Glia* **54**, 394–410.

Liu X, Wang Q, Haydar TF & Bordey A (2005). Nonsynaptic GABA signaling in postnatal subventricular zone controls proliferation of GFAP-expressing progenitors. *Nat Neurosci* **8**, 1179–1187.

Lledo PM, Alonso M & Grubb MS (2006). Adult neurogenesis and functional plasticity in neuronal circuits. *Nat Rev Neurosci* **7**, 179–193.

Merkle FT, Mirzadeh Z & Alvarez-Buylla A (2007). Mosaic organization of neural stem cells in the adult brain. *Science* **317**, 381–384.

More JC, Nistico R, Dolman NP, Clarke VR, Alt AJ, Ogden AM, Buelens FP, Troop HM, Kelland EE, Pilato F, Bleakman D, Bortolotto ZA, Collingridge GL & Jane DE (2004). Characterisation of UBP296: a novel, potent and selective kainate receptor antagonist. *Neuropharmacology* **47**, 46–64.

Nacher J, Crespo C & McEwen BS (2001). Doublecortin expression in the adult rat telencephalon. *Eur J Neurosci* **14**, 629–644.

Nam SC, Kim Y, Dryanovski D, Walker A, Goings G, Woolfrey K, Kang SS, Chu C, Chenn A, Erdelyi F, Szabo G, Hockberger P & Szele FG (2007). Dynamic features of postnatal subventricular zone cell motility: a two-photon time-lapse study. *J Comp Neurol* **505**, 190–208.

Paternain AV, Herrera MT, Nieto MA & Lerma J (2000). GluR5 and GluR6 kainate receptor subunits coexist in hippocampal neurons and coassemble to form functional receptors. *J Neurosci* **20**, 196–205.

Pinheiro P & Mulle C (2006). Kainate receptors. *Cell Tissue Res* **326**, 457–482.

Platel JC, Dave KA & Bordey A (2008). Control of neuroblast production and migration by converging GABA and glutamate signals in the postnatal forebrain. *J Physiol* **586**, 3739–3743.

Platel JC, Dupuis A, Boisseau S, Villaz M, Albrieux M & Brocard J (2007*a*). Synchrony of spontaneous calcium activity in mouse neocortex before synaptogenesis. *Eur J Neurosci* **25**, 920–928.

Platel JC, Lacar B & Bordey A (2007*b*). GABA and glutamate signaling: homeostatic control of adult forebrain neurogenesis. *J Mol Histol* **38**, 602–610.

Salt TE, Binns KE, Turner JP, Gasparini F & Kuhn R (1999). Antagonism of the mGlu5 agonist 2-chloro-5-hydroxyphenylglycine by the novel selective mGlu5 antagonist 6-methyl-2-(phenylethynyl)-pyridine (MPEP) in the thalamus. *Br J Pharmacol* **127**, 1057–1059.

Siegel SJ, Janssen WG, Tullai JW, Rogers SW, Moran T, Heinemann SF & Morrison JH (1995). Distribution of the excitatory amino acid receptor subunits GluR2(4) in monkey hippocampus and colocalization with subunits GluR5-7 and NMDAR1. *J Neurosci* **15**, 2707–2719.

Swanson GT, Feldmeyer D, Kaneda M & Cull-Candy SG (1996). Effect of RNA editing and subunit co-assembly single-channel properties of recombinant kainate receptors. *J Physiol* **492**, 129–142.

Vesikansa A, Sallert M, Taira T & Lauri SE (2007). Activation of kainate receptors controls the number of functional glutamatergic synapses in the area CA1 of rat hippocampus. *J Physiol* **583**, 145–157.

Wang DD, Krueger DD & Bordey A (2003*a*). Biophysical properties and ionic signature of neuronal progenitors of the postnatal subventricular zone *in situ*. *J Neurophysiol* **90**, 2291–2302.

Wang DD, Krueger DD & Bordey A (2003*b*). GABA depolarizes neuronal progenitors of the postnatal subventricular zone via $GABA_A$ receptor activation. *J Physiol* **550**, 785–800.

Acknowledgements

This work was supported by grants from the National Institutes of Health (NS048256 and DC007681, A.B.) and Yale Brown-Coxe fellowship (J.-C.P).

Supplemental material

Online supplemental material for this paper can be accessed at: http://jp.physoc.org/cgi/content/full/jphysiol.2008.155879/DC1